July 4, 1997

# Missing mass spectra in hadronic events at $\sqrt{s}$= 161–172 GeV and limits on invisible Higgs decays

The L3 Collaboration


## Abstract

Events characterised by large hadronic energy and transverse momentum are selected in the data collected by the L3 detector at LEP at centre of mass energies between 161 and 172 GeV, corresponding to an integrated luminosity of 21 pb$^{-1}$. The visible mass and the missing mass distributions of the selected events are consistent with the expected contributions from Standard Model processes. This result is combined with that of LEP 1 to set an upper limit on the production rate and decay into invisible final states of a non minimal Higgs boson, as function of the Higgs mass. Assuming the non minimal Higgs production cross section to be the same as for the Standard Model Higgs boson and the decay branching fraction into invisible final states to be 100%, a Higgs mass lower limit of 69.6 GeV is derived at 95% confidence level.


Submitted to the *XVIII International Symposium on Lepton-Photon Interactions*

# 1 Introduction

This paper reports on the results of a study of hadronic events, with large visible energy, visible mass and transverse momentum, in the data collected by the L3 experiment at $\sqrt{s}$ =161–172 GeV. The idea here is to tag events with a visible Z decaying hadronically recoiling against missing energy and momentum due to undetected particles. If a particle is produced in association with the Z and decays into invisible particles, then a peak in the missing mass spectrum should be observable. The kinematic region investigated here is different from those investigated in previous studies of hadronic events with missing energy and momentum, such as the one for the measurement of the $\mathrm{We}\nu$ cross section [1] as well as the $\mathrm{HZ} \to \mathrm{qq}\nu\nu$ search [2] and supersymmetric particle searches [3].

Non Standard Model processes could produce an unexpected excess of events in the spectrum of the missing mass recoiling to the Z. One example is the production of a non minimal Higgs boson, h, in association with a hadronically decaying Z boson and the Higgs decaying into invisible particles. In contrast, in the context of the Standard Model, the Higgs boson, H, decays always into visible final states, mainly $b$-quark pairs and $\tau$ lepton pairs. Examples of invisible particles which a non minimal Higgs could decay to are light neutralinos [4] in the context of supersymmetric extensions of the Standard Model; or Majorons [5], in so called Majoron models, used to generate neutrino masses.

In the following, the event selection is described and the data compared to the expectations for Standard Model processes. An excess of events is searched for in missing energy spectra, as it might be indicative of a Higgs produced in association with a Z boson and decaying into invisible particles.

# 2 Event topology

Invisible Higgs events, produced via the Higgs-strahlung process $\mathrm{e^+e^-} \to \mathrm{Zh}$, with $\mathrm{Z} \to \mathrm{q\bar{q}}$ and $\mathrm{h} \to$ invisible particles, and Standard Model Higgs events, produced via the same process, $\mathrm{e^+e^-} \to \mathrm{ZH}$, with $\mathrm{Z} \to \nu\bar{\nu}$ and $\mathrm{H} \to \mathrm{q\bar{q}}$, have similar signature: large visible energy, two acoplanar hadronic jets, large tranverse momentum and absence of isolated leptons. However, at present centre-of-mass energies, the Z boson is produced almost at rest, thus in invisible Higgs events the visible energy and visible mass are close to the Z mass, independently of the Higgs mass. This is not the case for Standard Model Higgs events, where the visible energy and visible masses are generally below the Z mass (in the Higgs mass range investigated at present energies), and depend upon the Higgs mass. Furthermore, in contrast to the Standard Model Higgs search, b-tagging is not efficient in selecting invisible Higgs events, since only about 15% of the total number of Higgs events will contain a $\mathrm{b\bar{b}}$ pair (from the Z) as compared to about 85 % of the total events in the SM Higgs events. Thus the analysis is based only on kinematic cuts and does not make use of b-tagging.

Hadronic events with large visible energy and momentum are originated also by Standard Model processes, such as quark pair production ($\mathrm{e^+e^-} \to \mathrm{q\bar{q}}(\gamma)$) and four fermion production, involving charged gauge boson exchange ( WW and We$\nu$ production) and neutral gauge boson exchange ( $Z/\gamma^*Z/\gamma^*$ and Zee production). The missing energy and momentum in these events is either genuine (e.g. in WW events, when one W decays into lepton+neutrino) or results from energy mismeasurement and incomplete detector coverage. The $q\bar{q}(\gamma)$ and WW events, mainly because of the relatively large size of their production rate (129 pb and 12.3 pb respectively for $q\bar{q}(\gamma)$ and WW cross sections at 172 GeV), are the most important sources of background in this search.

# 3 Data and Monte Carlo samples

For this analysis we use data corresponding to integrated luminosities of 10.8, 1.0 and 9.2 $pb^{-1}$ collected by the L3 detector [6] at LEP at centre-of-mass energies, $\sqrt{s}$, of 161.3, 170.3 and 172.3 GeV, respectively. For the signal efficiency studies a sample of Higgs events have been generated using PYTHIA [7], imposing 100% decay branching fraction of the Higgs boson into invisible particles. About 3.5K Higgs events, with hadronic Z decay, were simulated for Higgs mass value investigated. The Standard Model cross section for Higgs production is calculated using the HZHA generator [8]. For the study of fermion pair and four fermion productions the following Monte Carlo generators were used: PYTHIA ($e^+e^- \to q\bar{q}(\gamma)$), KORALW [9] ($e^+e^- \to W^+W^-$), PYTHIA and PHOJET [10] ($e^+e^- \to \gamma\gamma \to e^+e^-q\bar{q}$), and EXCALIBUR [11] ($e^+e^- \to f\bar{f}'f\bar{f}'$). The number of simulated fermion pair and four fermion events corresponds to at least 100 times the collected luminosity.

The L3 response is simulated using the GEANT 3.15 [12] program, which takes into account the effect of energy loss, multiple scattering and showering in the detector. The GHEISHA [13] program is used to simulate hadronic interactions in the detector.

# 4 Event selection

We first select hadronic events with large visible energy, with small parallel imbalance, and small energy in the forward calorimeters to suppress the $e^+e^- \to \gamma\gamma \to e^+e^-q\bar{q}$ contribution and reduce the $q\bar{q}(\gamma)$ contribution, with the photon in the forward region of the detector or escaping in the beam pipe. Then we apply additional requirements to further reduce the $q\bar{q}(\gamma)$ and WW contributions and select events with visible energy, momentum and mass consistent with a Z decaying into hadrons and recoiling against some undetected particle. As we reduce the event sample we compare the observed spectra of the visible mass, calculated from the visible energy $E_{\rm vis}$ and momentum $P_{\rm vis}$, $M_{\rm vis} = (E_{\rm vis}^2 - P_{\rm vis}^2)^{1/2}$ and the missing mass $M_{\rm mis} = (s + M_{vis}^2 - 2\sqrt{s}E_{vis})^{1/2}$, to the contributions from Standard Model fermion pair and four fermion productions.

The quantities used in the selection are: number of tracks $N_{\rm T}$; number of calorimetric clusters $N_{\rm C}$; the visible energy $E_{\rm vis}/\sqrt{s}$; parallel and perpendicular imbalances $|P_{\|}|/E_{\rm vis}$ and $P_{\perp}/E_{\rm vis}$; total energy deposition in the electromagnetic calorimeter (BGO) $E_{\rm BGO}$; energy deposition in the luminosity monitor $E_{LUM}$; energy deposition in the forward leadscintillator calorimeter (ALR) $E_{\rm ALR}$; relative energy in a cone of 30° around the beam direction, $E_{\rm v30}/E_{\rm vis}$; the larger of the two jet masses, $\max(M_{\rm j1}, M_{\rm j2})$, when the event is forced into two jets using DURHAM algorithm [14]; the sum of the angles between the jets, $\theta_{123}$, when the event is forced into three jets, using the DURHAM algorithm; the energy deposition in $\pm 25°$ of the missing momentum direction in the plane transverse to the beam, $E_{\rm t25}$; the number of high energy, isolated leptons, $N_{{\rm i}\ell}$, i.e. leptons $(e, \mu, \tau)$ with energy $E_l > 5$ GeV and isolation $I_\ell < 1$ GeV, where $I_l$ is the energy deposition in the region between 10 and 30 degrees half opening angle around the lepton direction.

The following cuts are applied in order to reduce the Standard Model contributions, mainly from $q\bar{q}(\gamma)$ and WW productions:

**Cut 1** Hadronic preselection: $N_{\rm C} > 14$, $N_{\rm T} > 4$, $E_{\rm BGO} > 10$ GeV, $E_{\rm LUM} < 5$ GeV, $E_{\rm ALR} < 10$ GeV, $0.4 < E_{\rm vis}/\sqrt{s} < 1$, $|P_{\parallel}|/E_{\rm vis} < 0.5$;

**Cut 2** $E_{\rm v30}/E_{\rm vis} < 0.5$;

**Cut 3** $E_{\rm vis}/\sqrt{s} < 0.7$;

**Cut 4** $|P_{\parallel}|/E_{\rm vis} < 0.3$;

**Cut 5** $\max(M_{\rm j1}, M_{\rm j2}) < 40$ GeV;

**Cut 6** $\theta_{123} < 349°$ for $\sqrt{s} = 172$ GeV or $\theta_{123} < 355°$ rad for $\sqrt{s} = 161$ GeV;

**Cut 7** $P_{\perp}/E_{\rm vis} > 0.1$ ;

**Cut 8** $N_{{\rm i}\ell} = 0$ and $E_{\rm t25} < 12$ GeV.

The distributions of the perpendicular imbalance, the maximum jet mass, the visible mass and the missing mass are shown in Figures 1(a) through 1(d) after the hadronic preselection (cut 1), for the data, the Standard Model expectation and, for comparison, a 70 GeV Higgs signal, at 172 GeV. At this centre-of-mass energy, after the hadronic preselection, 554 events are observed in the data, while 564 events are expected from Standard Model processes, of which 83% comes from $q\bar{q}\gamma$ production, 16% from WW production and the remainig 1% comes from Zee, $Z/\gamma^*Z/\gamma^*$ and $We\nu$ production. At $\sqrt{s} = 161$ GeV 791 events are observed with 778 expected from Standard Model processes with 96% from $q\bar{q}\gamma$, 3% from WW, and 1% from Zee, $Z/\gamma^*Z/\gamma^*$ and $We\nu$ production. The Higgs signal efficiency is 95%, with 5.1 events expected at 172 GeV and 1.2 at 161 GeV, for 70 GeV Higgs mass, assuming Standard Model cross section for Higgs production via $e^+e^- \rightarrow Zh$ process.

The selection progressively reduces the $q\bar{q}(\gamma)$ contribution and at a lesser extent the WW contribution. The most effective requirements to reduce the latter are the jet mass cut (cut 5), the $\theta_{123}$ angle cut (cut 6), the absence of isolated, high energy leptons and the isolation of the missing energy (cut 8). The jet mass cut and the $\theta_{123}$ angle cut, in particular, are very effective in reducing the WW contribution when one W decays hadronically and the other into a neutrino plus a tau. If the tau is not identified it is included in one of the two jets, when the event is reconstructed into two jets. Thus one of the two jet masses is high compared to genuine two-jet events. Similarly, when the $qq\tau\nu$ event is reconstructed into three jets it is likely to have a value of $\theta_{123}$ larger than for a genuine two jet event.

The number of events observed, as function of the selection cuts, compared to the SM predictions, is shown in Fig. 2. Good agreement between the data and the Standard Model expectations is found in the subsequent steps of the selection. For comparison, the numbers of events expected for an invisible Higgs signal , for two Higgs masses, assuming Standard Model ZH cross section, are also given.

In Fig. 3 the distributions of $M_{\mathrm{vis}}$ and $M_{\mathrm{mis}}$ after selection cuts 1 to 6 (see Fig. 2) are shown at centre-of-mass energies of 161 and 172 GeV. At this stage of the analysis, 21 events are observed in the data, while 20.7 events are expected from Standard Model processes, with 47% from $q\bar{q}\gamma$ events, 48% from WW events and 5% from Zee, $Z/\gamma^*Z/\gamma^*$ and $We\nu$ events. At $\sqrt{s}$ = 161 GeV 35 events are observed with 25.1 expected from Standard Model processes with the following composition: 81% $q\bar{q}\gamma$, 13% WW, and 6% from Zee, $Z/\gamma^*Z/\gamma^*$ and $We\nu$ production. The Higgs signal efficiency is 63% for a 65 GeV Higgs at $\sqrt{s}$=161 GeV and 62% for a Higgs mass of 70 GeV at $\sqrt{s}$=172 GeV and at 161 GeV.

For the Higgs events, the visible mass is close to the Z mass, with a Z mass resolution $\sigma_Z$ of about 9 GeV, and the missing mass is close to the Higgs mass, with a resolution which ranges from 15 to 12 GeV for Higgs masses between 60 and 70 GeV at 172 GeV. A better resolution in the Higgs mass is obtained imposing the constraint that the visible energy and momentum comes from the Z decay, and determining the Higgs energy from rescaling the measured missing energy, imposing total energy and momentum constraints. The expression for the reconstructed Higgs mass $M_{\mathrm{rh}}$ reads

$$M_{\mathrm{rh}} = \frac{\{\sqrt{s} - [s - (s - (M'_Z)^2)(1 - \beta^2_{\mathrm{mis}})]^{1/2}\}}{[1 - \beta^2_{\mathrm{mis}}]^{1/2}}$$

where $\beta_{\mathrm{mis}} = P_{\mathrm{vis}}/\sqrt{s} - E_{\mathrm{vis}}$ is, in the Higgs events, the measured Higgs velocity, and $M'_Z = M_Z + (M_{\mathrm{vis}} - M_Z)\Gamma_Z/\sigma_Z$, where $M_Z$ and $\Gamma_Z$ are the Z mass and the Z width, respectively. The improvement in Higgs mass resolution of $M_{\mathrm{rh}}$ as compared to $M_{\mathrm{mis}}$ is shown in Fig. 4, where the final selection (cuts 1 to 8) are applied. The distributions of $M_{\mathrm{vis}}$ and the reconstructed Higgs mass $M_{\mathrm{rh}}$ at $\sqrt{s}$= 161 and 172 GeV are shown for the data and the SM contributions and compared to the Higgs signal. The $M_{\mathrm{rh}}$ resolution ranges from 5.9 GeV for a 60 GeV Higgs to 3.6 GeV for a 70 GeV Higgs [15] at $\sqrt{s}$=172 GeV.

# 5 Results and conclusions

The observed number of events and the expected contributions from Standard Model processes, after final selection, are compared in Table 1. In total we expect 6.0±0.6 and

3.4±0.4 events from Standard Model physics processes and we observe 5 and 3 events at $\sqrt{s}$= 172 and 161 GeV, respectively. No excess in the data over the Standard Model expectations is detected.

The error on the Standard Model expectations includes the error from limited Monte Carlo statistics, which is 4% (see Table 1), and the error on the selection efficiency. This systematic uncertainty is mainly due to energy calibration uncertainties and it has been estimated by repeating the analysis with the global energy scale changed by ± 3% and the energy scales of the individual subdetectors by ±5 % [2]. It is estimated to be about 9%. Thus, a total error of about 10% is estimated to affect the Standard Model expectations.

The efficiencies for an invisibly decaying Higgs signal as a function of the Higgs mass are reported in Table 2 together with the number of $e^+e^- \rightarrow$ Zh events expected, assuming Standard Model Higgs production cross section, $\sigma(\mathrm{ZH_{SM}})$, and 100% branching fraction of the Higgs boson into invisible final states. A total error of about 4% affects the signal efficiencies, including both the uncertainty from limited Monte Carlo statistics ($\lesssim$ 2%) and the one due to energy calibration uncertainty (2.5 to 3.5% depending on the Higgs mass). The errors on the Higgs signal and background efficiencies are included in the calculation of the confidence level ([16]), using a gaussian smearing of the central values of the number of expected signal and background events, with standard deviations equal to the errors on signal and background expectations, discussed above.

Combining the 161–172 GeV results with those from LEP 1 [17], a 95% CL lower limit of 69.6 GeV (Fig. 5(a))is set on the mass of an invisibly decaying Higgs boson, assuming that the Higgs production cross section $\sigma$(Zh) is the same as for the Standard Model Higgs and the Higgs branching fraction into invisible particles, BR(h $\rightarrow$ invisible), is 100%.

The $e^+e^- \rightarrow$ Zh production cross section and the branching fraction into visible and invisible final states of a non standard Higgs boson h is model dependent. Thus we set an experimental upper limit, which can be used to bound the parameter space of the different models predicting invisible Higgs decays, on the rate of invisible Higgs final states, relative to the Standard Model Higgs rate, $R_{inv} = [\sigma(\mathrm{Zh})BR(\mathrm{h} \rightarrow \text{invisible particles})]/\sigma(\mathrm{ZH_{SM}})$, as a function of the Higgs mass. This is shown in Fig. 5(b) where the hatched area is excluded by L3 at 95% confidence level.

These results improve on those obtained in previous analyses at LEP 1 [17, 18, 19] and are the first ones reported at LEP 2 concerning invisible Higgs decays.

# Acknowledgements

We wish to express our gratitude to the CERN Accelerator Divisions for the good performance of the LEP machine. We acknowledge the efforts of the engineers and technicians who have participated in the construction and the maintenance of this experiment.

# References


[1] L3 Collaboration, M. Acciarri *et al.*, Production of Single W Bosons at LEP , CERN-PPE/97-28, in press on Phys. Lett. B.

[2] L3 Collaboration, "Search for the Standard Model Higgs Boson in $e^+e^-$ collisions at $161 \leq \sqrt{s} \leq 172$ GeV, in preparation.

[3] L3 Collaboration, "Searches for Supersymmetric Particles at $\sqrt{s}$ =161-172 GeV", in preparation.

[4] K. Griest, H.E. Haber, Phys. Rev. D 37 (1988) 719. A. Djouadi, P. Janot, J. Kalinowski (Warsaw U.), P.M. Zerwas, Phys. Lett. B 376 (1996) 220.

[5] A.S.Joshipura, J.W.F. Valle, Nucl. Phys. B 397 (1993) 105;
F. de Campos, O. J. Eboli, J. Rosiek, J. W. Valle, Phys. Rev. D 55 (1997) 1316.

[6] L3 Collaboration, B.Adeva *et al.*, Nucl.Instr.Meth. **A289** (1990) 35; J.A.Bakken *et al.*, Nucl.Instr.Meth. **A275** (1989) 81; O.Adriani *et al.*, Nucl.Instr.Meth. **A302** (1991) 53; B.Adeva *et al.*, Nucl.Instr.Meth. **A323** (1992) 109; K.Deiters *et al.*, Nucl.Instr.Meth. **A323** (1992) 162; M.Chemarin *et al.*, Nucl.Instr.Meth. **A349** (1994) 345; B.Acciari *et al.*, Nucl.Instr.Meth. **A351** (1994) 300; G.Basti *et al.*, Nucl.Instr.Meth. **A374** (1996) 293; A.Adam *et al.*, Nucl.Instr.Meth. **A383** (1996) 342.

[7] T.Sjöstrand, CERN-TH/7112/93 (1993), revised August 1995; T.Sjöstrand, Comp.Phys.Comm. 82 (1994) 74.

[8] P.Janot, "The HZHA generator", in "Physics at LEP2", Eds. G.Altarelli, T.Sjöstrand and F.Zwirner, CERN 96-01 (1996) Vol.2, 309.

[9] M.Skrzypek *et al.*, Comp.Phys.Comm. **94** (1996) 216; M.Skrzypek *et al.*, Phys.Lett. **B372** (1996) 289.

[10] R.Engel, Z.Phys. **C66** (1995) 203; R.Engel, J.Ranft and S.Roesler, Phys.Rev. **D52** (1995) 1459.

[11] F.A.Berends, R.Kleiss and R.Pittau, Nucl.Phys. **B 424** (1994) 308; Nucl.Phys. **B 426** (1994) 344; Nucl.Phys. (Proc. Suppl.) **B 37** (1994) 163; Phys.Lett. **B 335** (1994) 490; R.Kleiss and R.Pittau, Comp.Phys.Comm. **83** (1994) 14.

[12] R.Brun *et al.*, preprint CERN DD/EE/84-1 (Revised 1987).

[13] H.Fesefeldt, RWTH Aachen Report PITHA 85/02 (1985).

[14] S. Catani *et al.*, Phys. Lett. B 263 (1991) 491;
S. Bethke *et al.*, Phys. Lett. B (1992) 310.

[15] M. Felcini, L3 Higgs Working Group, L3 internal note 2073, March 97.

[16] V.F. Obratsov, Nucl. Instr. Meth. A 316 (1993) 388.

[17] L3 Collaboration, Phys. Lett. B 385 (1996) 454.

[18] OPAL Collaboration, Phys. Lett. B 377 (1996) 273.

[19] ALEPH Collaboration, Phys. Lett. B 313 (1993) 549.

| SM processes | $\sqrt{s}$=161 GeV | $\sqrt{s}$=172 GeV |
|---|---|---|
| $q\bar{q}$ | $1.15 \pm 0.13$ | $0.32 \pm 0.06$ |
| Zee | $0.003 \pm 0.002$ | $0.003 \pm 0.002$ |
| $Z/\gamma^{*}Z/\gamma^{*}$ | $0.028 \pm 0.007$ | $0.053 \pm 0.005$ |
| $We\nu$ | $0.90 \pm 0.05$ | $0.68 \pm 0.07$ |
| WW | $1.34 \pm 0.06$ | $5.02 \pm 0.11$ |
| Total expected | $3.40 \pm 0.15(stat)$ | $6.00 \pm 0.15(stat)$ |
| Total observed | 3 | 5 |

Table 1: The results of the selection, described in the text, on the data collected by the L3 experiment at CM energies between 161 and 172 GeV. The data sample corresponds to a luminosity of 10.7 and 10 $pb^{-1}$ respectively. The MC expectations are normalized to these luminosities using the SM cross sections. The quoted errors on the MC expectations are statistical only. The systematic errors are treated in the text.

| | LEP 1 | | $\sqrt{s}$=161 GeV | | $\sqrt{s}$=172 GeV | |
|---|---|---|---|---|---|---|
| Higgs mass (GeV) | $\epsilon_{Zh}(\%)$ | $N$ | $\epsilon_{Zh}(\%)$ | $N$ | $\epsilon_{Zh}(\%)$ | $N$ |
| 50 | 39 | 47.5 | 47 | 5.87 | 43 | 4.53 |
| 60 | 38 | 11.4 | 48 | 3.77 | 46 | 3.70 |
| 65 | 36 | 4.55 | 42 | 2.10 | 47 | 3.15 |
| 67 | 35 | 2.99 | 37 | 1.36 | 48 | 2.94 |
| 69 | 33 | 1.87 | 29 | 0.581 | 45 | 2.48 |
| 70 | 32 | 1.46 | 28 | 0.362 | 46 | 2.40 |
| 71 | 31 | 1.12 | 27 | 0.230 | 45 | 2.11 |
| 73 | 30 | 0.64 | 24 | 0.100 | 45 | 1.87 |

Table 2: Efficiencies, after the selection described in the text, for the Zh signal, with the Higgs decaying invisibly and the Z decaying hadronically. They are affected by a 4% total uncertainty. The number of expected Higgs events N predicted by the SM (calculated with the HZHA program [8]) for the ZH production processes, are also given. The efficiencies for LEP 1 are affected by a 3% total uncertainty [17]. The LEP 1 data used are those used in the analysis described in [17].

## Figure Captions

Fig. 1: Distributions, at $\sqrt{\mathrm{s}} = 172$ GeV, after the hadronic preselection, of (a) the perpendicular imbalance, (b) the maximum jet mass, when the event is reconstructed into two jets, (c) the visible mass and (d) the missing mass. Events with $\mathrm{M}^2_{\mathrm{mis}} \leq 0$ (due to measurement errors) are plotted with $\mathrm{M}_{\mathrm{mis}} = 0$. The data (black dots) are compared to the sum of the SM contributions (empty histogram) for fermion pair production plus four fermion production. Superimposed (hatched histogram) are the distributions for a 70 GeV Higgs mass. Here the Higgs distribution are normalized to 10 times the actual luminosity using the Standard Model ZH production cross section.

Fig. 2: The number of events observed in the data at (a) $\sqrt{\mathrm{s}} = 172$ GeV and (b) $\sqrt{\mathrm{s}} = 161$ GeV, compared to the expectations for SM production of fermion pairs plus four fermion final states. The number of events expected for a Higgs of 70 GeV at $\sqrt{\mathrm{s}} = 172$ and of 65 GeV at $\sqrt{\mathrm{s}} = 161$ are also shown. The Higgs distributions are normalized to the actual luminosities using the SM ZH production cross section.

Fig. 3: Distributions of the visible mass and the missing mass after selection cut 6 (see fig. 2) at $\sqrt{\mathrm{s}} = 172$ GeV and at $\sqrt{\mathrm{s}} = 161$ GeV for the data compared to the sum of the SM processes and the signal distributions for 65 GeV. The Higgs distributions are normalized to the actual luminosities at the two CM energies, using the SM ZH production cross section.

Fig. 4: Distributions of (a) the visible mass $\mathrm{M}_{\mathrm{vis}}$ and (b) the reconstructed Higgs mass $\mathrm{M}_{\mathrm{rh}}$ at $\sqrt{\mathrm{s}} = 172$ GeV and (c) and (d) at $\sqrt{s}$= 161 GeV. The data (black dots) are compared to the sum of the SM contributions (empty histogram). All the distributions are normalized to the luminosities collected at center of mass energies of 172 and 161 GeV. Superimposed are the same distributions for a signal of a 70 GeV Higgs for $\sqrt{\mathrm{s}} = 172$ GeV and 65 GeV Higgs for $\sqrt{\mathrm{s}} = 161$ GeV. The Higgs distributions are normalized to the actual luminosities at the two CM energies, using the SM ZH production cross section.

Fig. 5: Lower limit on the invisible Higgs mass, assuming SM Higgs production cross section and 100% decay branching ratio into invisible particles, and $\mathrm{R}_{\mathrm{inv}} = [\sigma(\mathrm{Zh})\mathrm{BR}(\mathrm{h} \rightarrow \mathrm{invisible})]/\sigma(\mathrm{ZH}_{\mathrm{SM}})$.

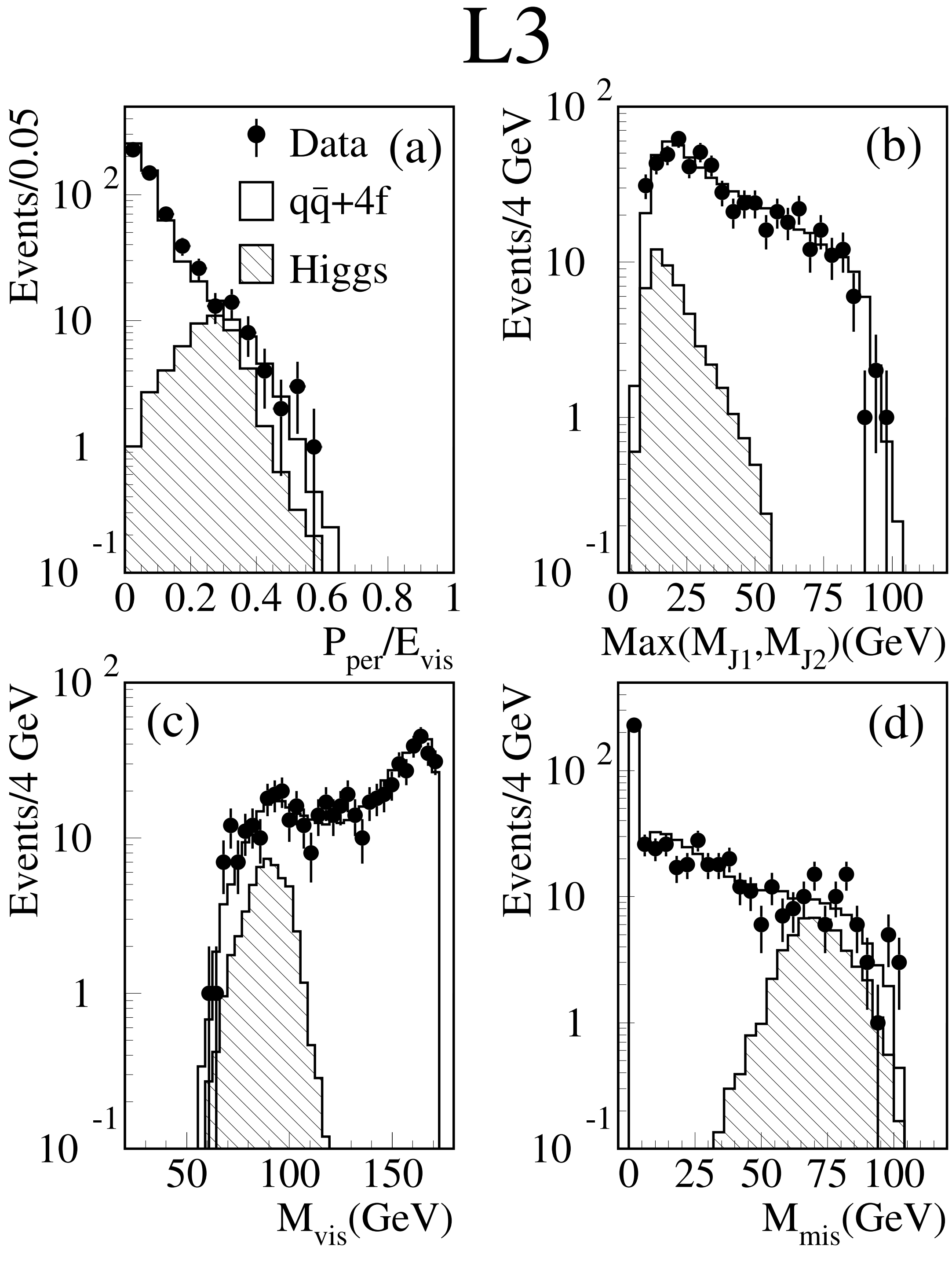

L3
Data
(a)
q$\bar{q}$+4f
Higgs
Events/0.05
$P_{per}/E_{vis}$
(b)
Events/4 GeV
$Max(M_{J1},M_{J2})$(GeV)
(c)
Events/4 GeV
$M_{vis}$(GeV)
(d)
Events/4 GeV
$M_{mis}$(GeV)

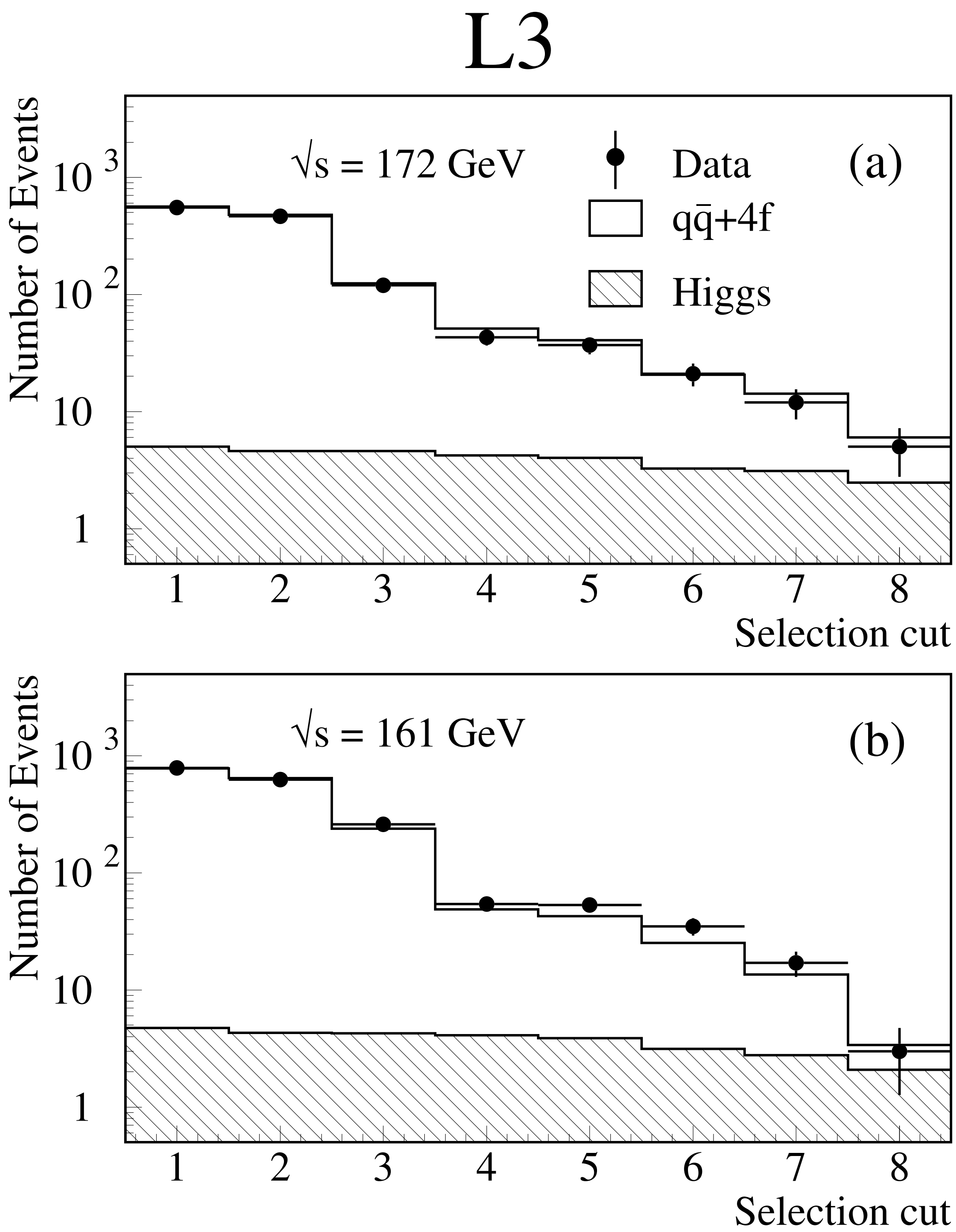
L3
Number of Events
√s = 172 GeV
Data
qq̄+4f
Higgs
(a)
Selection cut
√s = 161 GeV
(b)
Selection cut

**Figure 2**

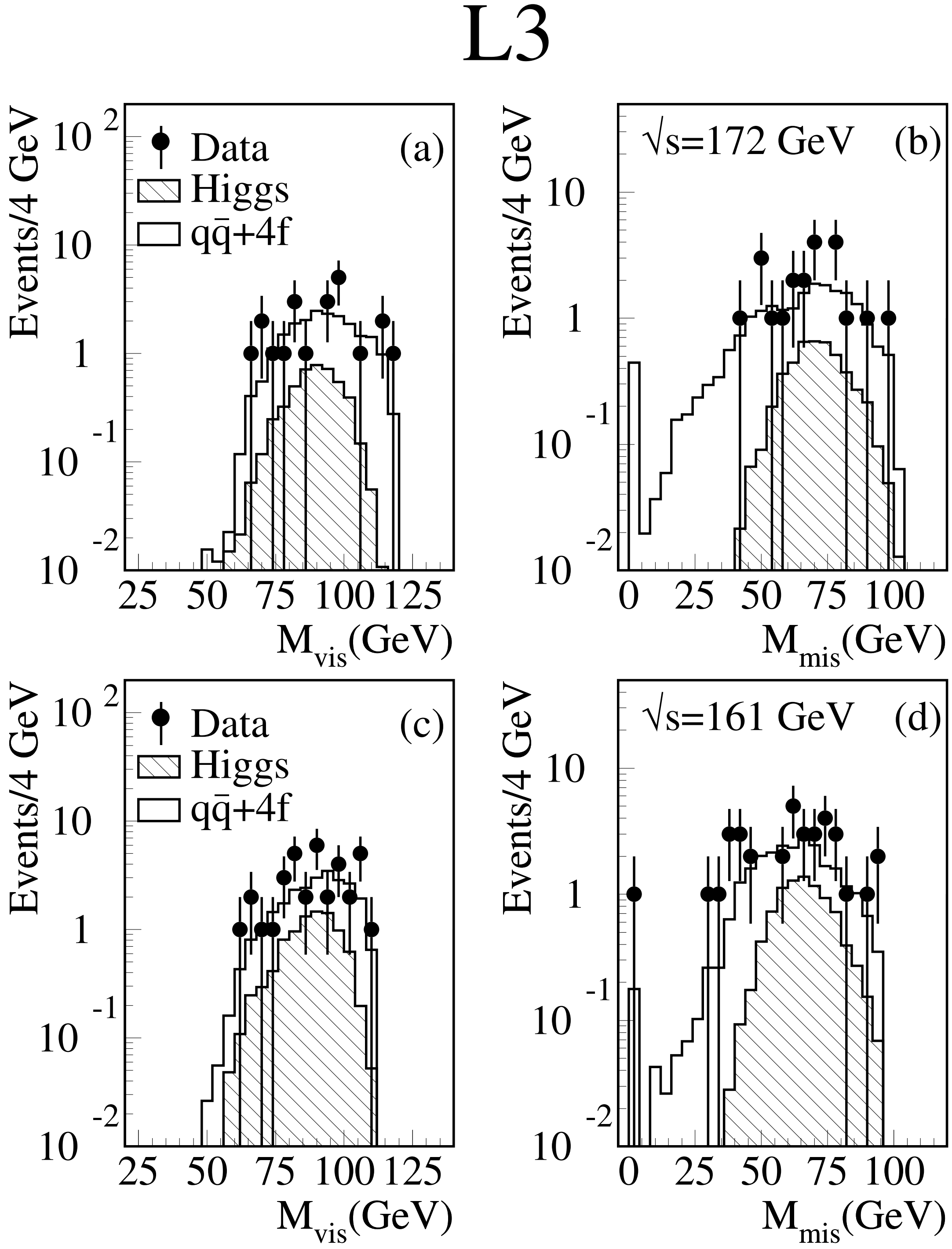
L3
Events/4 GeV
Data
(a)
Higgs
q$\bar{q}$+4f
$M_{vis}$(GeV)
√s=172 GeV
(b)
$M_{mis}$(GeV)
(c)
√s=161 GeV
(d)

**Figure 3**

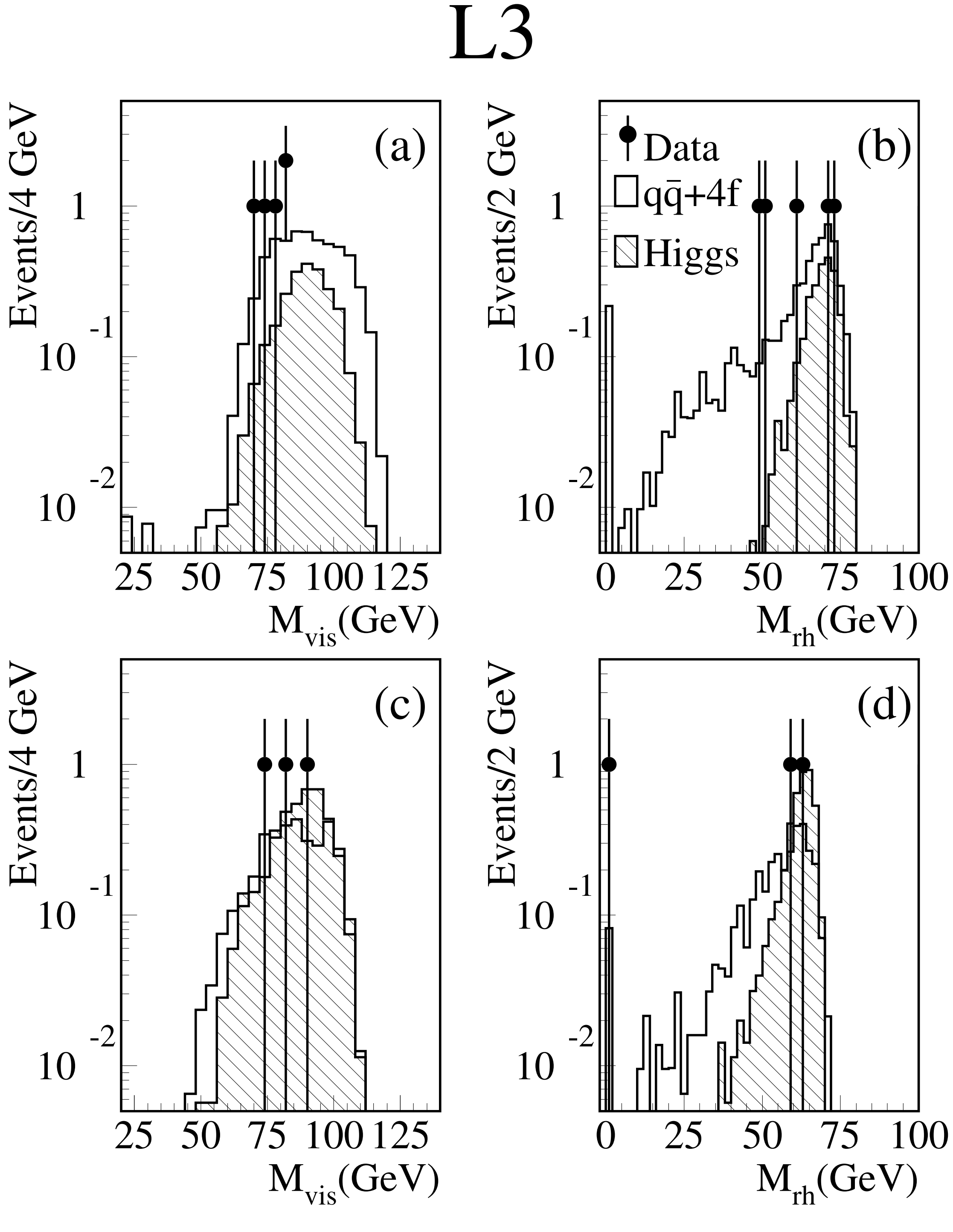
L3
(a)
Events/4 GeV
1
$10^{-1}$
$10^{-2}$
25 50 75 100 125
$M_{vis}$(GeV)
(b)
Data
$q\bar{q}$+4f
Higgs
Events/2 GeV
0 25 50 75 100
$M_{rh}$(GeV)
(c)
Events/4 GeV
$M_{vis}$(GeV)
(d)
Events/2 GeV
$M_{rh}$(GeV)

**Figure 4**

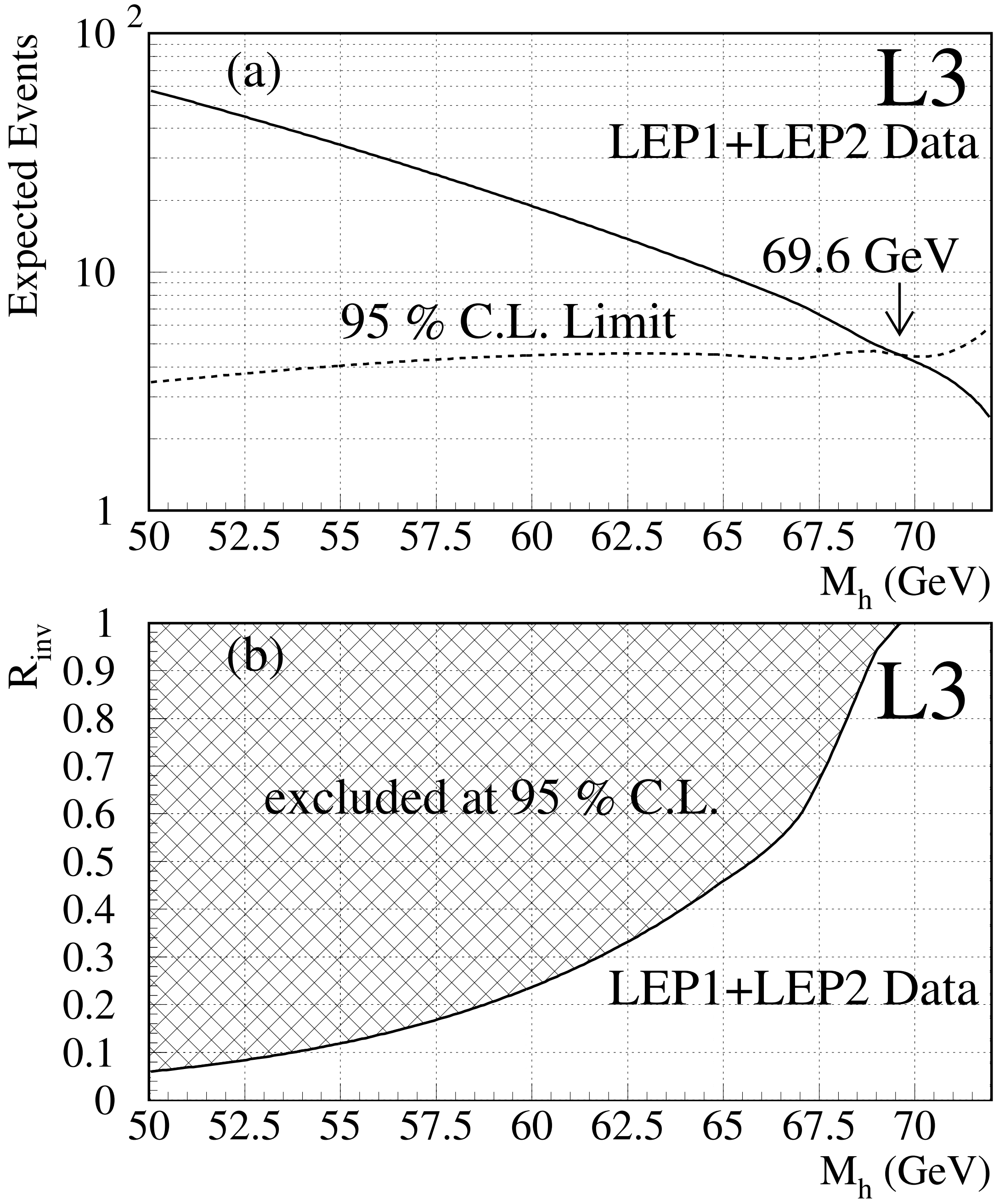

(a)
L3
LEP1+LEP2 Data
69.6 GeV
95 % C.L. Limit
Expected Events
10 2
10
1
50
52.5
55
57.5
60
62.5
65
67.5
70
M h (GeV)
(b)
L3
excluded at 95 % C.L.
LEP1+LEP2 Data
R inv
1
0.9
0.8
0.7
0.6
0.5
0.4
0.3
0.2
0.1
0
50
52.5
55
57.5
60
62.5
65
67.5
70
M h (GeV)


**Figure 5**